

## A Scheme to Identify Loops from Trajectories of Oceanic Surface Drifters: An Application in the Kuroshio Extension Region

CHANGMING DONG,\* YU LIU,<sup>+,#</sup> RICK LUMPKIN,<sup>@</sup> MATTHIAS LANKHORST,<sup>&</sup> DAKE CHEN,\*\*  
JAMES C. MCWILLIAMS,\* YUPING GUAN<sup>+</sup>

<sup>\*</sup> *Institute of Geophysics and Planetary Physics, University of California, Los Angeles, Los Angeles, California*

<sup>+</sup> *Key Laboratory of Tropic Marine Environment Dynamics, South China Sea Institute of Oceanology, CAS, Guangzhou, China*

<sup>#</sup> *Graduate University of Chinese Academy of Sciences, Beijing, China*

<sup>@</sup> *NOAA/Atlantic Oceanographic and Meteorological Laboratory, Miami, Florida*

<sup>&</sup> *Scripps Institution of Oceanography, La Jolla, California*

<sup>\*\*</sup> *State Key Laboratory of Satellite Oceanic Environment and Dynamics, SIO/SOA, Hangzhou, China*

(Manuscript received 12 November 2010, in final form 11 April 2011)

### ABSTRACT

When a drifter is trapped in an eddy, it makes either a cycloidal or a looping trajectory. The former case takes place when the translating speed is larger than the eddy spinning speed. When the background mean velocity is removed, drifter trajectories make loops. Thus, eddies can be detected from a drifter trajectory by identifying looping segments. In this paper, an automated scheme is developed to identify looping segments from Lagrangian trajectories, based on a geometric definition of a loop, that is, a closing curve with its starting point overlapped by its ending point. The scheme is to find the first returning point, if it exists, along a trajectory of a surface drifter with a few other criteria. To further increase the chance that detected loops are eddies, it is considered that a loop identifies an eddy only when the loop's spinning period is longer than the local inertial period and shorter than the seasonal scale, and that at least two consecutive loops with the same polarity that stay sufficiently close are found. Five parameters that characterize an eddy are estimated by the scheme: location (eddy center), time (starting and ending time), period, polarity, and intensity. As an example, the scheme is applied to surface drifters in the Kuroshio Extension region. Results indicate that numbers of eddies are symmetrically distributed for cyclonic and anticyclonic eddies, mean eddy sizes are 40–50 km, and eddy abundance is the highest along the Kuroshio path with more cyclonic eddies along its southern flank.

### 1. Introduction

A Lagrangian eddy detection scheme for oceanic surface drifters seeks to identify a looping segment within a trajectory. Manual detection of “loopers” has been conducted in many studies (e.g., Richardson 1993; Shoosmith et al. 2005; Fratantoni and Richardson 2006). For example, Richardson (1993) made the first statistical census of eddies from Lagrangian trajectory data. He collected over 230 sound fixing and ranging floats during 1972–89 and manually identified eddies from the float trajectories. However, manual detection is time consuming and subject to human error or bias. There are a

few automated eddy detection algorithms in the literature, for example, Glenn and Ebbesmeyer (1993), Boebel et al. (2003), Griffa et al. (2008), Lankhorst (2006), Lilly and Gascard (2006), Hamilton et al. (1999), Beron-Vera <sup>AU1</sup> et al. (2008), and Lilly and Olhede (2010). These methods may be categorized into the following four types:

- 1) Lagrangian stochastic model (LSM) based: Griffa et al. (2008) calculated spin rates from a trajectory based on a two-dimensional and first-order LSM (Veneziani et al. (2005a,b)). When the spin rate <sup>AU2</sup> surpasses a nonzero threshold, the segment is an eddy; Lankhorst (2006) used a second-order autoregression (AR) to identify a segment as an eddy, in which two velocity components have similar frequencies, durations, and persistence. The method is actually a second-order, one-dimensional LSM-based approach.

*Corresponding author address:* Dr. Changming Dong, Institute of Geophysics and Planetary Physics, University of California, Los Angeles, Los Angeles, CA 90095.  
E-mail: cdong@atmos.ucla.edu.

- 2) Ellipse pattern recognition: Studies include the work of Glenn and Ebbesmeyer (1993), Hamilton et al. (1999), Lilly and Gascard (2006), and Lilly and Olhede (2010). Using an ellipse divergence model, Glenn and Ebbesmeyer (1993), Hamilton et al. (1999), and Hamilton (2007) identified eddies from smoothed drifter paths. Lilly and Gascard (2006) and Lilly and Olhede (2010) applied a wavelet technique to time-varying trajectories to detect ellipses.
- 3) Lagrangian dynamical system tool: Beron-Vera et al. (2008) extracted Lagrangian coherent structures (LCSs) from finite-time Lyapunov exponent fields, and these LCSs delineate fluid domains with different advective properties; thus, their detection provides eddy boundaries.
- 4) Geometric approach: Boebel et al. (2003) calculated the curvature of a trajectory to determine whether an eddy exists.
- 3) For higher-frequency processes, such as inertial oscillations, a drifter makes loops. For lower-frequency processes, such as basin-scale gyre rotation, a loop is also possible. We consider the Lagrangian eddy frequency to be between the intraseasonal scale and slower than the inertial scale, thus we apply a period criteria to only select loops in this period range.
- 4) To make a conservative selection, looping is considered to be an eddy only if two or more consecutive loops with the same polarity are found along the same drifter's trajectory. This condition will exclude eddies associated with a single loop in the drifter trajectory.

In this paper, we introduce a simple automated loop-identifying scheme (ALIS), which is based on a geometric definition of a loop; here, a loop is a closed and continuous curve with its starting point overlapped by its ending point or, in other words, a drifter returns to its former position after some time. When the idea is implemented in practice to realistic sea surface drifters for eddy identification, the following conditions need to be added:

- 1) Because observational data or numerical products of a drifter's trajectory are always discrete data, when a drifter returns exactly to its former point, it is almost certainly not recorded in its trajectory data and so we can only expect that it comes within some threshold distance to a former point. The threshold distance needs to be defined first and the definition varies from data to data because it is determined by the temporal interval of data sampling and velocity, and practically it is estimated using the mean spatial interval from a trajectory.
- 2) Even if the drifter "returns" based on the definition of the threshold distance, it could be a cluster of points that stays around the point and does not make a loop (spinning), so that a rotating angle is calculated in the scheme: only when the trajectory makes a complete enclosed curve can the segment be considered a loop.

As stated above, the purpose of ALIS is to identify eddies from the drifter trajectories. With the above two conditions, loops can be identified. However, not all loops are eddies. The following two additional conditions are applied to filter out those loops that are not eddies:

Finally, it should be noted that when the background velocity (large-scale flow) exceeds the spinning speed of an eddy, a trapped drifter traces a cycloidal trajectory, not a closed loop. This can happen in an ocean, such as with the core of the Kuroshio, which is in the region selected here as a test bed for ALIS. Thus, to avoid missing eddies that have trapped drifters, a preprocessing procedure is applied to the data: the drifter trajectories in a frame of reference moving with the time-mean current. However, in reality, we do not know the exact mean flow. Though two methods are suggested herein, the accurate mean flow is unknown. The inaccuracy in the estimation of the mean flow could cause some errors in the detection. Thus, the preprocessing scheme is provided in the ALIS package; however, it is an option.

Because ALIS is based on geometric features of a loop, it is different from the first three types of schemes and thus is categorized as type 4. It is also different from the scheme of Boebel et al. (2003), which is also based on the geometry of a loop, but uses curvature to identify loops.

The ALIS scheme is implemented in MATLAB language and is easy to use. Section 2 of this paper provides a detailed description of the scheme; sections 3 and 4 are an application and discussion, respectively.

## 2. Methodology

When a drifter makes a loop in its trajectory, it implies that the drifter returns to a point it passed some time ago. To automatically detect such a "returning" segment from a drifter trajectory and estimate eddy characteristics thus measured by the drifter, we develop a scheme including the following four steps described below.

### a. Step 1: Identification looping segments

We define a drifter returning to a former position as follows: when a distance between the current position and a former point is less than a threshold distance  $D_0$ ,

we consider that the drifter has returned to the former position. The threshold distance  $D_0$  can be estimated as the multiplication of a background velocity with a sampling time interval. If a trajectory dataset is evenly sampled in time, then in practical terms we can use averaged spatial intervals from trajectories in the region.

Consider a trajectory  $\Gamma$ , consisting of a series of points  $P(i)$ , where  $i = 1, \dots, M$ , and  $M$  is the total number of samples in  $\Gamma$ . Here,  $D(i, j)$  is the distance between point  $P(i)$  and point  $P(j)$ . At one point  $P(i)$ , we search the first point  $P(k)$  whose distance from  $P(i)$ ,  $D(i, k)$ , is less than  $D_0$ . The searching range is  $[i + \tau, \min(i + N, M)]$ , where  $\tau$  is a cut-off time step number for the removal of high-frequency oscillations, and  $N$  is the maximum number of time steps to search a loop, which is the longest loop spinning period expected for an eddy in the region. In other words, if the number of steps needed to return to  $P(i)$  exceeds  $N$ , then the scheme stops searching and the scheme moves to next point  $P(i + 1)$ . Thus, if found,  $P(k)$  satisfies the following conditions:

$$D(i, k) \leq D_0, \quad i + \tau < k < \min(i + N, M), \quad (1)$$

where  $D(i, k)$  is the distance between  $P(i)$  and  $P(k)$ . All of the points from  $P(i)$  to  $P(k)$  are recorded as the points that form a loop. The interval of time the drifter takes to move from  $P(i)$  to  $P(k)$  is the loop period. The averaged position of all the points from  $P(i)$  to  $P(k)$  is the center of the loop. The scheme then moves to the next point  $P(k + 1)$  to repeat the procedure to look for a new loop. If neither a loop starting at point  $P(i)$  is found or the condition (1) is not satisfied, then it proceeds to the next point  $P(i + 1)$  to repeat the above procedure to check if there is a loop starting from  $P(i + 1)$ . After the procedure is applied to all of the points along the trajectory  $\Gamma$ , that is, the index  $i$  goes from 1 to  $M$ , then all of the loops existing along the trajectory  $\Gamma$  can be detected automatically.

#### b. Step II: Rotating angle and the polarity of a loop

With a loop identified from a trajectory, its spinning direction, that is, eddy polarity, needs to be determined as clockwise or counterclockwise. When a drifter follows an anticyclonic eddy in the Northern (Southern) Hemisphere, it makes a clockwise (counterclockwise) loop. To determine the spinning direction of the loop, we calculate a total angle  $\Theta$  with which a vector, pointing from the center of the loop to each point along the loop, completes its starting point to its ending point along the loop. As an example, Fig. 1 shows positions of the vector in green at each time step when the drifter makes a loop. Generally, the total angle  $\Theta$  the vector makes is close to

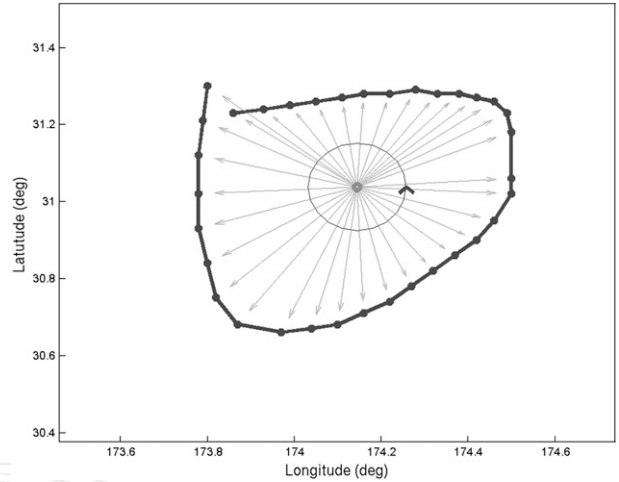


FIG. 1. An example shows how ALIS determines the polarity of a loop. A segment of the trajectory of a drifter 7711687 from the GDP data (the number is the drifter ID) is shown (thick blue line). The position of the geometric center of the loop is shown (red circle). Points from the loop center to each sampling point along the loop are shown (green vectors). The direction of the loop spins are shown (blue arrow in a small circle).

$360^\circ$ , and it is either clockwise (negative) or counterclockwise (positive). The sign of the angle is the polarity of an eddy presented by the loop.

It is still possible that a cluster of points will satisfy condition 1 but will not be a loop. For example, see Fig. 2, where two small segments are marked A and B, where the drifter wobbles almost in the same location (meeting condition 1) but does not make a closing curve spinning around a center. To eliminate these, we use the rotating angle obtained from this step to further check the segment. If the angle  $\Theta$  is larger than a minimum angle  $\Theta_0$  (a default is set to be  $300^\circ$ ), then the segment can be considered a loop,

$$\Theta > \Theta_0. \quad (2)$$

Figure 2 shows two examples of two clockwise and counterclockwise loops detected by the ALIS scheme. In the right panel of Fig. 2, for example, two small closed segments marked as A and B are not recorded as loops.

#### c. Step III: Parameters of a loop

In step I, we identify loops from a trajectory in which we have determined loop centers, time (starting and ending time), and the loop spinning period. In step II, the polarity of the loop is estimated by using a radiating vector pointing to the points along the loop. The length of the radiating vectors  $\mathbf{R}$  can be considered the size of the loop. We choose the averaged length of the vectors that go through all points along the loop (see Fig. 1) as

AU3

F1

F2



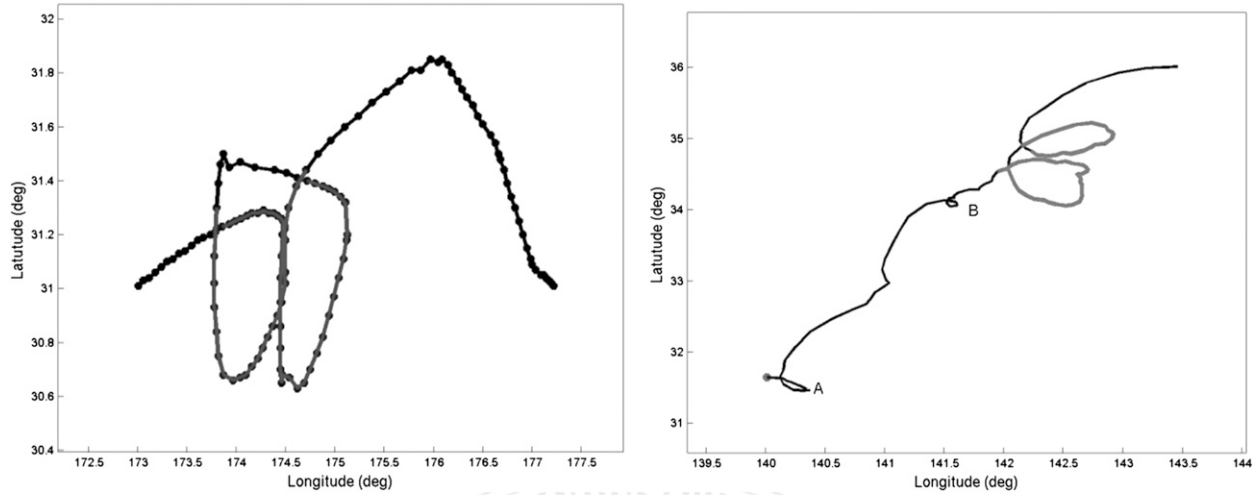


FIG. 2. Examples of loops detected using ALIS. (left) Two clockwise loops detected from the trajectory of drifter 7711687 are shown. (right) Two counterclockwise loops detected from the trajectory of drifter 75631 are shown. The drifters' trajectories (black lines) are shown, as are the counterclockwise (blue) and clockwise (red) loops. (left) The small loops marked A and B are loops whose frequencies are higher than the cut-off frequency and not recorded as loops by ALIS.

the size of the loop. The eccentricity of the eddy can be estimated using the series of radical vectors

$$\varepsilon = [\max(r) - \min(r)] / [\max(r) + \min(r)], \quad (3)$$

where  $r$  is the scalar of the vector  $\mathbf{R}$ .

The loop intensity can be described as the vorticity of an eddy the loop represents, defined as

$$\Omega = \text{sign}(\Theta)U/\text{avg}(r), \quad (4)$$

where  $U$  is the mean tangential speed, which is the speed averaged over all of the points of the loop,  $\text{avg}(r)$  is averaged  $r$  (the loop size), and  $\Theta$  is the total angle a radical vector completes through the loop.

Thus far we have obtained five parameters of a loop: location (center), time (starting and ending time), spinning period, polarity, and intensity, which describe the primary characteristics of an eddy the loop represents.

#### d. Step IV. Tracking an eddy

The three steps described above can automatically identify all of the explicit loops along a trajectory of a drifter and also provide five parameters characterizing an eddy or eddies creating the loops. While most drifters do not follow an eddy for its entire lifetime, identifying a group of loops associated with a single eddy can provide at least partial information of an eddy evolution. In this step we introduce a way to group all loops that track the same eddy using location and time information. We check whether

- 1) two temporally neighboring loops are in the same polarity, and
- 2) the distance between the two loops is within an advection distance by the ambient oceanic current. The ambient mean current can be obtained by averaging over all the points along two loops. The advection distance is the time interval between the two loops multiplied by the mean current.

When these two criteria are met, the two loops can be considered as tracking the same eddy. Then the procedure can be extended to the next loop to check if the third loop, if it exists, also belongs to the same eddy. Figure 2 shows examples of two continuous loops tracking the same eddy.

Four parameters need to be assigned with numbers before the ALIS detection scheme can be used. In step 2, the minimum rotating angle  $\Theta$  can be assigned the value of  $300^\circ$ , which can be used in all cases, so it is not listed below. Two more parameters are chosen as follows:

- 1) The threshold distance  $D_0$  for defining a drifter as returning to its former point. With an oceanic current scale  $U_0$ , and the time interval for drifter sampling  $\Delta t$ , the distance between two adjacent points  $\Delta t U_0$  is a grid size scale resolved by the drifter. Considering the search procedure goes through each point, we choose the grid distance as the criteria distance,

$$D_0 = \alpha \Delta t U_0, \quad (5)$$

where  $0 < \alpha < 1$ , a default value is set to be 0.5. Practically, an averaged grid size shall be used [the

grid size is defined as a distance  $D(i, i + 1)$ , where the index  $i$  goes through all the time steps if time steps are uniform].

- 2) A cut-off time step  $\tau$ , which is used for the removal of the inertial oscillation, which can be determined by the local inertial frequency  $f = 2\Omega \sin(A)$ , where  $\Omega$  is the earth rotating frequency ( $\Omega = 2\pi/24 \text{ h} = 7.28 \times 10^{-5} \text{ s}^{-1}$ ),  $A$  is the latitude where the search starts, and so

$$\tau = \text{int}[\beta \Delta t / (2\pi/f)], \quad (6)$$

where  $\beta$  is an adjusting factor, a default value is 2.0.

In summary, there are four steps for detecting loops using the ALIS. Five parameters characterizing each loop are estimated: location, time (starting and ending time), period, polarity, intensity, and eccentricity. Loops tracking the same eddy can be grouped. There are three parameters that need to be assigned.

Thus, the ALIS scheme can identify looping segments from trajectories. However, not all loops are eddies. For example, high-frequency processes, such as inertial oscillations, can make loops, and low-frequency processes, such as basin-scale gyre flow, can also make a large-scale loop. To remove these loops, we exclude loops with periods larger than that of the local inertial period or smaller than an intraseasonal scale (i.e., maximum loop searching time is 90 days in step 1). Furthermore, only when at least two consecutive loops with the same polarity are found along the same drifter's trajectory and the two loops are close enough (within the advection distance) are the two loops considered as eddies. Practically speaking, only loops meeting these two additional conditions are considered to be eddies.

ALIS is coded in MATLAB. The ALIS package will be released online to the community.<sup>1</sup>

### 3. Application to Kuroshio Extension region

#### a. Data

In this section, we use historical surface drifter data to test the above scheme. The data are maintained by the Global Drifter Program (GDP; see Lumpkin and Pazos 2007). The GDP drifters have widely been used for the estimation of global oceanic circulation and other oceanic dynamical and climatological studies (e.g., Niiler and Paduan 1995; Hansen and Poulain 1996; Niiler 2001; Niiler et al. 2003; data are available online at

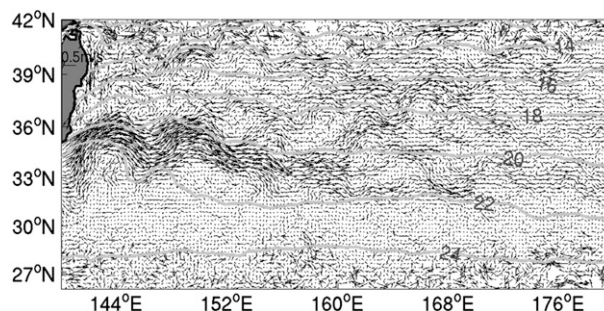


FIG. 3. Mean velocity vectors derived from the surface drifter trajectories averaged in  $1/4^\circ$  bins. Contours are the 2006–08 mean SST from REMSS SST data.

<http://www.aoml.noaa.gov/phod/dac/dacdata.html>). The drifters drogued at a depth of 15 m to follow near-surface currents are collected for this study. The data include the location and hydrographic variables, and they are evenly mapped at an interval of 6 h. There are data from over 13 000 global drifters from 1979 to the present maintained by the GDP.

#### b. General analysis

The Kuroshio Extension (KE) region is chosen as a test bed. The domain is  $(30^\circ\text{N}, 40^\circ\text{N}) \times (139^\circ\text{E}, 182^\circ\text{E})$ . After the Kuroshio separates from the east coast of Japan, the Kuroshio becomes a free eastward jet and is unstable. Thus, the KE has long been recognized as a region that is rich in energetic pinched-off eddies (see Qiu and Chen 2010 for a review). For this study, all of the drifters with at least part of their trajectories falling in the KE domain are selected. Therefore, some drifters might have some parts of their trajectories in the domain and some outside the domain. There are in total 475 drifters in KE region as of March 2009. Figure 3 plots the mean currents derived from the GDP drifter data, which shows a meandering Kuroshio path after it leaves the shelf (Niiler et al. 2003), which also demonstrates that the drifter data density is a sufficient trajectory to characterize the flow in the KE region [an eddy kinetic energy (EKE) distribution can be seen in Fig. 4]. The mean sea surface temperature (SST) is superimposed on the mean velocity field in Fig. 3. The SST data are from the Remote Sensing System (downloaded from <http://www.remss.com>). The resolution of the SST data is 9 km. This shows that the Kuroshio is located between  $20^\circ$  and  $\sim 22^\circ\text{C}$ .

Before the ALIS scheme is applied to the drifter data in the KE, a general Lagrangian analysis is conducted using the data (Lankhorst and Zenk 2006). The EKE is high in the KE region, as shown on the upper-left panel

<sup>1</sup> This will be made available once the final manuscript is accepted for publication.

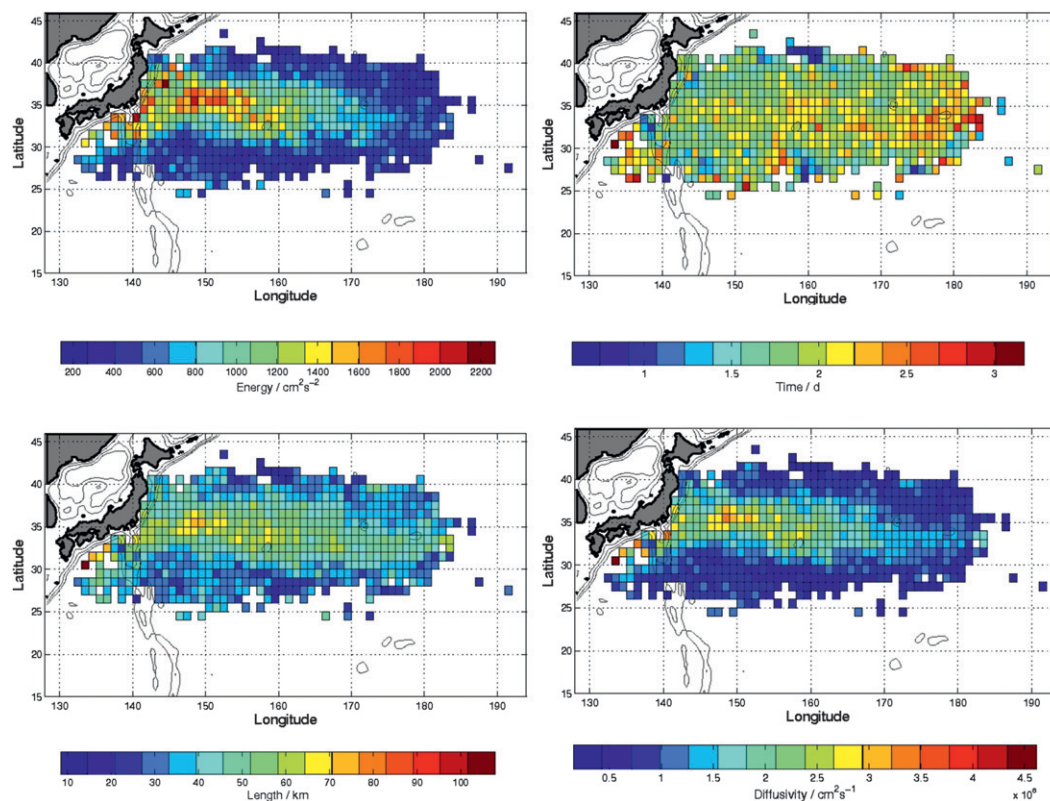


FIG. 4. (top left) Eddy kinetic energy, (top right) Lagrangian integral time, (bottom left) Lagrangian length scale, and (bottom right) Lagrangian eddy diffusivity. All derived from GDP drifters.

of Fig. 4. The EKE is calculated by subtracting the mean current from each velocity. The Lagrangian integral time scale, which characterizes the decorrelation scale between the two components of the velocities, is plotted on the upper-right panel, which reflects the eddy time scale. Using the EKE and the Lagrangian integral time, one can estimate the so-called Lagrangian length scale by  $t \times \sqrt{\text{EKE}}$  and the Lagrangian eddy diffusivity as  $K_v = \text{EKE} \times t$ , assuming homogeneous and isotropic turbulence (Lumpkin et al. 2002). The Lagrangian length scale is plotted in the lower-left panel of Fig. 4 with values ranging over 50–100 km. This scale is comparable to the size of eddies detected by ALIS (see section 3d).

### c. Statistical results of eddies detected by ALIS

In a realistic ocean, a trajectory of a drifter could be very complicated. Figure 5 shows an example of a drifter trajectory that includes many loops, which are highlighted with colors. From the marked segments, one can tell that ALIS is capable of detecting these explicit loops. Note that not all of these loops are associated with eddies; noneddy closed loops can be removed using the criteria discussed earlier.

Thus far we assume that all eddies can be explicitly identified as closed loops in drifter trajectories. However, if the background current magnitude is larger than an eddy's tangential speed, then a drifter within an eddy does not complete a loop in fixed geographical coordinates, but instead traces a cycloid. Generally, oceanic eddies have much higher kinetic energy than the mean current, except in narrow regions such as western boundary currents, such as the KE region; thus, in most cases, we can use the scheme directly. However, to make the ALIS globally applicable, we introduce a preprocessing step to the scheme: we remove the background current (mean current) and reconstruct Lagrangian trajectories in the frame of reference moving at the mean current speed. Although we do not have accurate information of the time-varying background velocities, we may use mean velocities averaged over all of the drifters available as an approximation. That is why in the current application we choose a region with a strong current to test the scheme. In the KE region, the mean velocity is shown in Fig. 3. With mean velocities removed from the velocities recorded in the drifter data, we reconstruct all of the trajectories with the following formula:



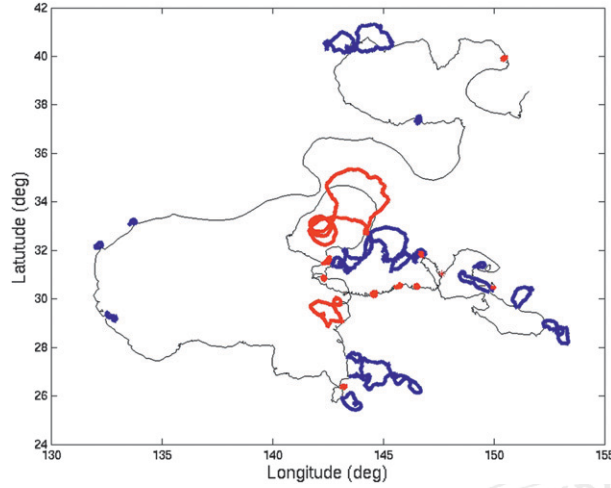


FIG. 5. A drifter trajectory example showing the complexity of a realistic drifter trajectory. The trajectory of drifter 18951 is shown (black line), as is the counterclockwise (blue) and clockwise (red) loop identified by ALIS. As described in the text, not all of these closed loops are identified as eddies.

$$\begin{aligned} X'(t) &= X(t) - \int_0^t u[X(t), Y(t)] dt, \\ Y'(t) &= Y(t) - \int_0^t v[X(t), Y(t)] dt, \end{aligned} \quad (7)$$

where  $(X, Y)$  and  $(X', Y')$  are locations of the original and reconstructed trajectories, respectively, and  $(u, v)$  is the mean velocity. In section 4, the impact of removing the mean velocity affects is presented.

For the KE region, we choose the threshold distance as 5 km, the cut-off period as 1 day, and the maximum search time as 90 days. In total 2179 loops are detected. When only two consecutive loops that stay close enough (within the mean advection distance) with the same polarity and from the same drifter's trajectory are counted as eddies, then 2058 eddies are identified. In the following, a statistical analysis is applied to these eddies detected by ALIS. Among the 2058 eddies, there are 970 cyclonic and 1088 anticyclonic eddies, which is about 10% more anticyclonic than cyclonic eddies. To examine the eddy size distribution, the histogram of eddy size is plotted in the upper panel of Fig. 6. The histogram peaks at 30–40 km for anticyclonic and cyclonic eddies. It should be pointed out that eddy sizes estimated from drifters' trajectories are usually underestimated because drifters could be well inside of an eddy. Actually, the eddy sizes estimated from drifter data are lower limits of eddy sizes. The peak of eddy number in the eddy size histogram is the lower limit of the Lagrangian length scale (40–100 km) in Fig. 4.

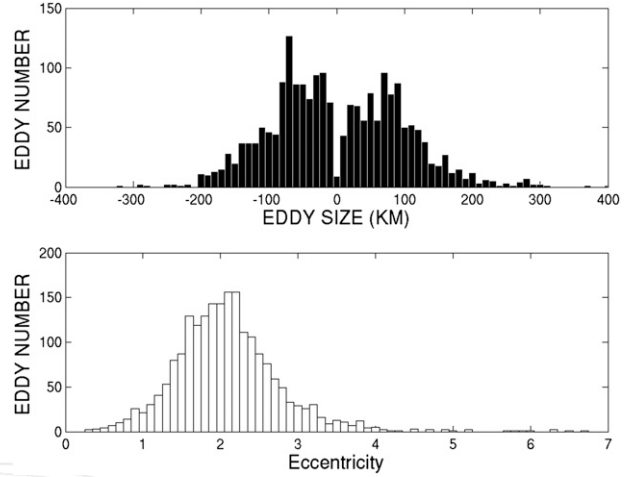


FIG. 6. (top) Histogram of loop sizes with a bin width of 5 km. Negative sizes are for anticyclonic eddies while positive sizes for cyclonic eddies. (bottom) Histogram of loop eccentricity with a bin width of 0.25.

AU14

Some argue that cyclonic eddies in the ocean may be undersampled by drifters because of the diverging flow but, on the other hand, drifters tend to be at a certain depth, so in a sense they can only feel the nondivergent part of the flow (M. Veneziani ???, personal communication). Figure 6 shows that more anticyclonic eddies are detected by the drifter trajectories in the KE region. Itoh and Yasuda (2010) examined the SSHA data in an extended KE region and also found more anticyclonic eddies than cyclonic eddies with lifetimes longer than 12 weeks, but almost equal numbers with lifetimes longer than 54 weeks. The lower panel of Fig. 6 shows the eccentricity of loops, which is defined as the rate of the difference between the long axis and short axis, and the averaged length of the two axes. When the eccentricity is zero, the shape of a loop is circular while a larger eccentricity implies a deformed eddy. The peak of the eccentricity histogram is at an eccentricity of 2.0.

AU10

Figure 7 plots the histograms of eddy vorticity and eddy temperature recorded by the drifters. Vorticity is normalized by the background Coriolis parameter  $f$ . The histograms peaks are at about  $0.025f$ . The peak temperature of the loops are about  $20^{\circ}$ – $22^{\circ}$ C for both cyclonic and anticyclonic eddies, which demonstrates that most eddies are in the Kuroshio path by comparison with the SST distribution (Fig. 3). This is also seen in Fig. 8, which shows the spatial distribution of cyclonic and anticyclonic eddy numbers in  $0.5^{\circ} \times 0.5^{\circ}$  bins.

F7

F8

#### 4. Discussion and summary

In the preprocessing step, large-scale mean currents in a region are removed and new trajectories are

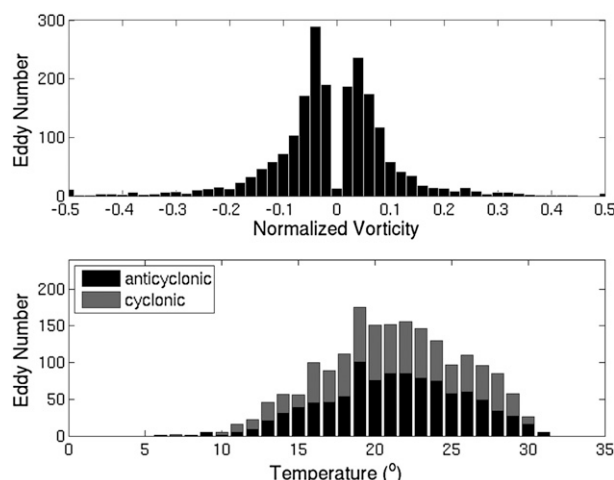


FIG. 7. (top) Histogram of eddy vorticity and (bottom) histogram of the mean water temperature recorded by drifters within eddies.

reconstructed. To test how the removal of the mean affects the results, we also apply the scheme directly to the original trajectory data without removing the mean. In total, 1808 eddies are detected when mean velocities are not removed (963 anticyclonic and 845 cyclonic loops). In contrast, 2058 loops are identified with mean velocities removed (1088 cyclonic and 970 anticyclonic eddies), so there are about 10% more loops detected in the reconstructed Lagrangian trajectories. Figure 9 plots the number of eddies in each latitude strip (a strip with is 1°) both with and without mean velocities removed. There are more eddies identified in the former case along the Kuroshio main axis located in 33°–35°N, with more cyclonic eddies on the southern edge of the Kuroshio and more anticyclonic eddies in the northern part of the Kuroshio. More eddies are identified because some drifters that are trapped in the eddies within the Kuroshio jet do not make closed loops because of the strong current. However, when the mean current is removed, those loops can be identified.

As with any automatic eddy detection schemes, either from Eulerian or Lagrangian data, there are always some uncertainties associated with assigned values to parameters. In this scheme, for example, we consider the choice of a threshold distance. A decrease in this distance could include higher-frequency oscillations as loops while an increase in this distance could result in some small eddies being missed. For the choice of the longest search time (90 days herein), a longer search time might result in a trajectory segment of a flow gyre that is taken as an eddy; a shorter search time might exclude some eddies that have a long rotating period. In section 2, we have given some general rules for choosing such numbers based on their physical meaning, that is,

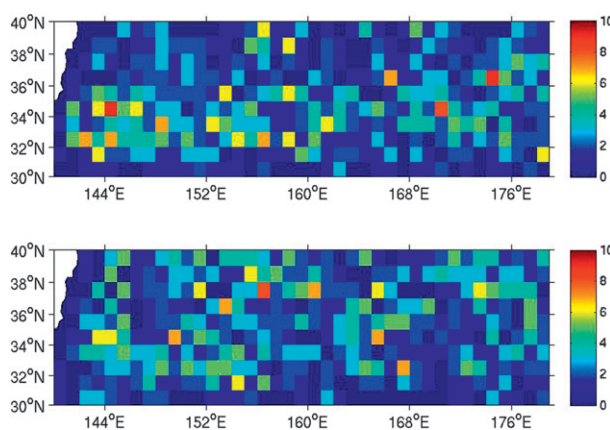


FIG. 8. Eddy number distribution in  $1^\circ \times 1^\circ$  bins: (top) cyclonic and (bottom) anticyclonic.

a range of the values for these parameters. Within such certain ranges, there are no significant differences in the statistical results of detected eddies in the KE region.

As stated above, only if at least two consecutive loops with the same polarity are found along the same drifter's trajectory are the loops considered eddies. Although this condition might be conservative (which could exclude a single loop that is an eddy), only 10% of the loops do not meet the condition in the KE region. The best way to check whether a loop is an eddy is to cross-check with other data available. We show an example of the comparison of this Lagrangian eddy detection scheme with the Eulerian eddy detection scheme, such as with the sea surface height anomaly (SSHA) data by altimetry and SST data, in Fig. 10. The presence of a cyclonic eddy is

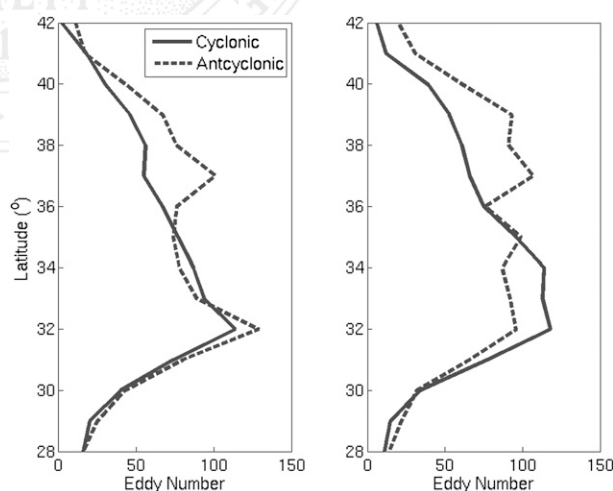


FIG. 9. Eddy number distribution as function of latitude (solid lines are for cyclonic eddies and dashed lines for anticyclonic eddies). (left) Original data and (right) reconstructed data with mean velocities removed.



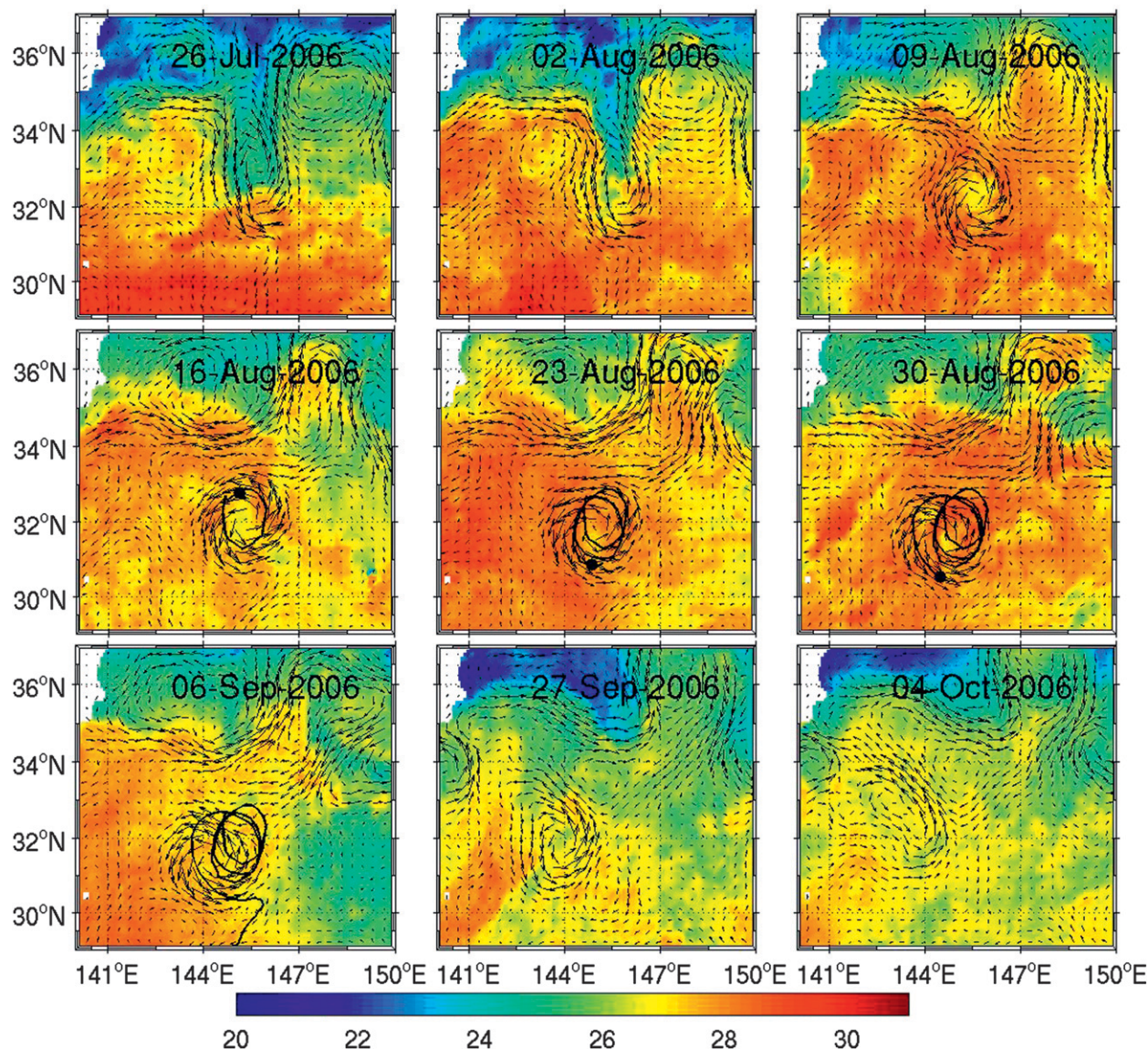


FIG. 10. An example showing a drifter looping within an eddy. The trajectory of GDP drifter 62309 is shown (black curve). The time is marked on each panel. The vectors are geostrophic velocity anomalies from altimetry data. The color is the SST data from REMSS SST data. The current location of the drifter is indicated (black dots).

well confirmed by both the SSHA and SST data. Part of the eddy life time is tracked by a drifter (ID 62309). One can also see other eddies that are not tracked by drifters. It is a very interesting topic to make a cross comparison among eddies detected by SSHA, SST, or drifters, but this is beyond the scope of the current paper.

In summary, the automated eddy detection scheme ALIS is introduced in this paper with an application to surface drifter trajectory data in a region with high kinetic energy: the Kuroshio Extension region. A pre-processing step is suggested to be taken first to reconstruct Lagrangian trajectories by removing background currents

when a strong background current is present. Mean currents averaged over velocities from all of the drifter data are used. Four steps are conducted to identify a looping segment from a drifter trajectory and estimate five parameters of the eddy: 1) to determine a loop segment using a definition of returning point and rotating angle close to 360°; 2) to estimate the polarity of an eddy; 3) to estimate size, vorticity, and period eddy parameters; and 4) to track an eddy. Only loops with an intraseasonal spinning period and two consecutive loops with the same polarity close enough along the same drifter's trajectory are considered as eddies. The ALIS

MATLAB code package will be released online in conjunction with publication of the paper.

**Acknowledgments.** CD appreciates support from the National Science Foundation (OCE 06-23011) and the National Aeronautics and Space Administration (Grant NNX08AI84G). YL and YPG are supported by the National Basic Research Program of China (2007CB411801). During the preparation of the work, CD had extensive discussions with Drs. Jonathan Lilly, Milena Veneziani, and Carter Ohlmann, and their comments are much appreciated.

# REFERENCES

- Beron-Vera, F. J., M. J. Olascoaga, and G. J. Goni, 2008: Oceanic mesoscale eddies as revealed by Lagrangian coherent structures. *Geophys. Res. Lett.*, **35**, L12603, doi:10.1029/2008GL033957.
- Boebel, O., J. Lutjeharms, C. Schmid, W. Zenk, T. Rossby, and C. Barron, 2003: The Cape Caudron: A regime of turbulent inter-ocean exchange. *Deep-Sea Res. II*, **50**, 57–86.
- Fratantoni, D. M., and P. L. Richardson, 2006: The evolution and demise of North Brazil Current Rings. *J. Phys. Oceanogr.*, **36**, 1241–1264.
- Glenn, S. M., and C. C. Ebbesmeyer, 1993: Drifting buoy observations of a loop current anticyclonic eddy. *J. Geophys. Res.*, **98**, 20 105–20 119.
- Griffa, A., R. Lumpkin, and M. Veneziani, 2008: Cyclonic and anticyclonic motion in the upper ocean. *Geophys. Res. Lett.*, **35**, L01608, doi:10.1029/2007GL032100.
- Hamilton, P., 2007: Eddy statistics from Lagrangian drifters and hydrography for the northern Gulf of Mexico slope. *J. Geophys. Res.*, **112**, C09002, doi:10.1029/2006JC003988.
- , G. S. Fargion, and D. C. Biggs, 1999: Loop Current eddy paths in the western Gulf of Mexico. *J. Phys. Oceanogr.*, **29**, 1180–1207.
- Hansen, D. V., and P. M. Poulain, 1996: Quality control and interpolations of WOCE-TOGA drifter data. *J. Atmos. Oceanic Technol.*, **13**, 900–909.
- Itoh, S., and I. Yasuda, 2010: Characteristics of mesoscale eddies in the Kuroshio–Oyashio Extension region detected from the distribution of the sea surface height anomaly. *J. Phys. Oceanogr.*, **40**, 1018–1034.
- Lankhorst, M., 2006: A self-contained identification scheme for eddies in drifter and float trajectories. *J. Atmos. Oceanic Technol.*, **23**, 1583–1592.
- , and W. Zenk, 2006: Lagrangian observations of the middepth and deep velocity fields of the northeastern Atlantic Ocean. *J. Phys. Oceanogr.*, **36**, 43–63.
- Lilly, J. M., and J.-C. Gascard, 2006: Wavelet ridge diagnosis of time-varying elliptical application to an oceanic eddy. *Non-linear Processes Geophys.*, **13**, 467–483.
- , and S. C. Olhede, 2010: Bivariate instantaneous frequency and bandwidth. *IEEE Trans. Signal Process.*, **58**, 591–603.
- Lumpkin, R., and M. Pazos, 2007: Measuring surface currents with Surface Velocity Program drifters: The instrument, its data, and some recent results. *Lagrangian Analysis and Prediction of Coastal and Ocean Dynamics*, A. Griffa et al., Eds., Cambridge University Press, xx–xx.
- , A.-M. Treguier, and K. Speer, 2002: Lagrangian eddy scales in the northern Atlantic Ocean. *J. Phys. Oceanogr.*, **32**, 2425–2440.
- Niiler, P., 2001: The world ocean surface circulation. *Ocean Circulation and Climate*, G. Siedler, J. Church, and J. Gould, Eds., International Geophysics Series, Vol. 77, Academic Press, 193–204.
- , and J. D. Paduan, 1995: Wind-driven motions in the northeast Pacific measured by Lagrangian drifters. *J. Phys. Oceanogr.*, **25**, 2819–2830.
- Niiler, P. P., N. A. Maximenko, and J. C. McWilliams, 2003a: Dynamically balanced absolute sea level of the global ocean derived from near-surface velocity observations. *Geophys. Res. Lett.*, **30**, 2164, doi:10.1029/2003GL018628.
- , —, G. G. Panteleev, T. Yamagata, and D. B. Olson, 2003b: Near-surface dynamical structure of the Kuroshio Extension. *J. Geophys. Res.*, **108** (C6), 3193, doi:10.1029/2002JC001461.
- Qiu, B., and S. Chen, 2010: Eddy-mean flow interaction in the decadally-modulating Kuroshio Extension system. *Deep-Sea Res.*, **57**, doi:10.1016/j.dsr2.2008.11.036.
- Richardson, P. L., 1993: A census of eddies observed in North Atlantic SOFAR float data. *Prog. Oceanogr.*, **31**, 1–50.
- Shoosmith, D. R., P. L. Richardson, A. S. Bower, and H. T. Rossby, 2005: Discrete eddies in the northern North Atlantic as observed by looping RAFOS floats. *Deep-Sea Res. II*, **52**, 627–650.

AU12

AU13